Molecular Pharmacology Fast Forward. Published on June 17, 2009 as doi:10.1124/mol.109.057489
This article has not been copyedited and formatted. The final version may differ from this version.



# 15-Oxo-Eicosatetraenoic Acid, a Metabolite of Macrophage 15-Hydroxyprostaglandin Dehydrogenase that Inhibits Endothelial Cell Proliferation

Cong Wei, Peijuan Zhu, Sumit J. Shah, and Ian A. Blair

Centers for Cancer Pharmacology and Excellence in Environmental Toxicology, University of Pennsylvania School of Medicine, 854 BRB II/III, 421 Curie Boulevard, Philadelphia, PA 19104-6160

Molecular Pharmacology Fast Forward. Published on June 17, 2009 as DOI: 10.1124/mol.109.057489
This article has not been copyedited and formatted. The final version may differ from this version.



**Running title: 15-Oxo-Eicosatrienoic Acid Inhibits Endothelial Proliferation**

Address correspondence to Dr. Ian A. Blair Center for Cancer Pharmacology, University of Pennsylvania, 854 BRB II/III, 421 Curie Boulevard, Philadelphia, PA 19104-6160, (tel.) 215-573-9885, (fax) 215-573-9889, (e-mail) ianblair@mail.med.upenn.edu. (phone) 215-573-9880.

**ABBREVIATIONS:** 15d-$PGJ_2$, 15-deoxy-$\Delta^{12,14}$-prostaglandin $J_2$; 15-HETE, 15-hydroxy-5,8,11,13-(*Z*,*Z*,*Z*,*E*)-eicosatetraenoic acid; 15-HPETE, 15-hydroperoxy-5,8,11,13-(*Z*,*Z*,*Z*,*E*)-eicosatetraenoic acid; 5-oxo-ETE, 5-oxo-6,8,11,14-(*E*,*Z*,*Z*,*Z*)-eicosatetraenoic acid, 15-oxo-ETE, 15-oxo-5,8,11,13-(*Z*,*Z*,*Z*,*E*)-eicosatetraenoic acid; AA, arachidonic acid; BrdU, 5-bromo-2-deoxyuridine; CAY10397, 5-[[4-ethoxycarbonyl) phenyl)azo]-2-hydroxy-benzeneacetic acid; CDC, cinnamyl-3,4-dihydroxy-α-cyanocinnamate; CI , calcium ionophore A-23187; $cPLA_2$, cytosolic phospholipase $A_2$; DMEM, Dulbecco's Modified Eagle's Medium; EC, endothelial cell; ECAPCI, electron capture atmospheric pressure chemical ionization; ELISA, Enzyme-linked immunosorbent assay; FBS, fetal bovine serum; GGTP, γ-glutamyltranspeptidase; HUVEC, human umbilical vein endothelial cells; IL, interleukin; JAK1, Janus kinase 1; LC, liquid chromatography; LO, lipoxygenase; MRM, multiple reaction monitoring; MS, mass spectrometry; OEG, 15-oxo-ETE-GSH adduct; OEC, 15-oxo-ETE-cysteinyl-adduct; PBS, phosphate buffered saline; PFB, 2,3,4,5,6-pentafluorobenzyl; PG, prostaglandin; PGDH, hydroxyprostaglandin dehydrogenase; PPAR, peroxisome proliferator-activated receptor; R15L cells, mouse macrophage RAW cells stably expressing human 15-LO-1; ROS; RMock cells, mouse macrophage RAW cells transfected with the pcDNA3 plasmid; rt, retention time. Stat6, signal transducer and activator of transcription 6.

Number of Text Pages: 32

Number of Figures: 9

Number of References: 40

Words in Abstract: 238 (250 max)

Words in Introduction: 605 (750 max)

Words in Discussion: 1309 (1500 max)

Molecular Pharmacology Fast Forward. Published on June 17, 2009 as DOI: 10.1124/mol.109.057489
This article has not been copyedited and formatted. The final version may differ from this version.



## ABSTRACT

The formation of 15-oxo-5,8,11,13-(*Z*,*Z*,*Z*,*E*)-eicosatetraenoic acid (15-oxo-ETE) as a product from rabbit lung 15-hydroxyprostaglandin dehydrogenase (PGDH)-mediated oxidation of 15(*S*)-hydroperoxy-5,8,11,13-(*Z*,*Z*,*Z*,*E*)-eicosatetraenoic acid (15(*S*)-HPETE) was first reported over 30-years ago. However, the pharmacological significance of 15-oxo-ETE formation has never been established. We have now evaluated 15-lipoxygenase (LO)-1-mediated arachidonic acid (AA) metabolism to 15-oxo-ETE in human monocytes and mouse RAW macrophages that stably express human 15-LO-1 (R15L cells). A targeted lipidomics approach was employed to identify and quantify the oxidized lipids that were formed. 15-oxo-ETE was found to be a major AA-derived LO metabolite when AA was given exogenously or released from endogenous esterified lipid stores by calcium ionophore A-23187 (CI). This established the R15L cells as a useful *in vitro* model system. Pre-treatment of the R15L cells with cinnamyl-3,4-dihydroxycyanocinnamate (CDC), significantly inhibited AA- or CI-mediated production of 15(*S*)-hydroperoxy-5,8,11,13-(*Z*,*Z*,*Z*,*E*)-eicosatetraenoic acid (15(*S*)-HETE) and 15-oxo-ETE, confirming the role of 15-LO-1 in mediating AA metabolite formation. Furthermore, 15(*S*)-HETE was metabolized primarily to 15-oxo-ETE. Pre-treatment of the R15L cells with the 15-PGDH inhibitor, 5-[[4-ethoxycarbonyl) phenyl]azo]-2-hydroxy-benzeneacetic acid (CAY10397), reduced AA- and 15(*S*)-HETE-mediated formation of 15-oxo-ETE in a dose-dependent manner. This confirmed that macrophage-derived 15-PGDH was responsible for catalyzing the conversion of 15(*S*)-HETE to 15-oxo-ETE. Finally, 15-oxo-ETE was shown to inhibit the proliferation of human vascular vein endothelial cells (HUVECs) by suppressing DNA synthesis, implicating a potential anti-angiogenic role. This is the first report describing the biosynthesis of 15-oxo-ETE by macrophage/monocytes and its ability to inhibit endothelial (EC) proliferation.

Molecular Pharmacology Fast Forward. Published on June 17, 2009 as DOI: 10.1124/mol.109.057489
This article has not been copyedited and formatted. The final version may differ from this version.



## Introduction

15-oxo-ETE was originally shown to arise from rabbit lung 15-PGDH-mediated oxidation of 15(*S*)-HETE (Bergholte et al., 1987) (Fig. 1). More recently, 15-oxo-ETE was identified as a metabolite of COX-2-mediated-AA metabolism (Lee et al., 2007). It was also observed as an AA metabolite formed in human mast cells (Gulliksson et al., 2007). Unlike its 5-LO-derived isomer, 5-oxo-6,8,11,14-(*E,Z,Z,Z*)-eicosatetraenoic acid (5-oxo-ETE), the pharmacology of 15-oxo-ETE has not been explored in detail (Murphy and Zarini, 2002; Powell and Rokach, 2005). Therefore, this interesting AA metabolite has remained a pharmacological curiosity for many years. AA is present in many esterified lipid classes and can be released by the action of specific lipases. It can then be oxidized to lipid hydroperoxides either enzymatically by COXs (Blair, 2008) and LOs (Jian et al., 2009) or non-enzymatically by the action of reactive oxygen species (Porter et al., 1995).

Bioactive lipid mediators are increasingly being recognized as important endogenous regulators of angiogenesis (Gonzalez-Periz and Claria, 2007). One of the major cascades of bioactive lipid mediator production involves the release of AA from membrane phospholipids followed by COX-2-mediated formation of eicosanoids (Lee et al., 2007). Eicosanoids produced by COX-2 are thought to promote tumorigenesis by stimulating angiogenesis (Cha et al., 2006). It is noteworthy that there is an increased level of lipid peroxidation in atherosclerotic lesions as evidenced by the presence of lipid hydroperoxide-derived bifunctional electrophiles such as 4-hydroxy-2-nonenal (as a pyrrole derivative) (Salomon et al., 2000).

In contrast to 5-LOs, which strongly prefer free AA as substrate (Jian et al., 2009), mammalian 15-LOs are capable of oxygenating both free and esterified polyunsaturated fatty acids (Kühn and O'Donnell, 2006). 15-LO can also oxygenate even more complex lipid-protein

Molecular Pharmacology Fast Forward. Published on June 17, 2009 as DOI: 10.1124/mol.109.057489
This article has not been copyedited and formatted. The final version may differ from this version.



assemblies such as biomembranes (Kühn and Borchert, 2002) and lipoproteins (Brinckmann et al., 1998). Type 1 human 15-LO (15-LO-1), mainly expressed by reticulocytes, eosinophils and macrophages, is the enzyme responsible for converting AA to 15(*S*)-HPETE and a small amount of 12(*S*)-hydroperoxy-5,8,10,14-(*Z*,*Z*,*E*,*Z*)-eicosatetraenoic acid; (Bryant et al., 1982). 15-LO-1 is a cytoplasmic enzyme with up-regulated expression in atherosclerotic lesions and localization at sites of macrophage accumulation (Kühn and Chan, 1997). Studies of 15-LO-1 in hematopoietic cells have demonstrated that it translocates to the inner plasma membrane and other non-nuclear membranes (e.g. sub-mitochondrial membranes) after stimulation with calcium (Walther et al., 2004).

Endothelial cells are activated by murine macrophage 12/15-LO activity in the presence of low-density lipoprotein (Huo et al., 2004). Furthermore, it has been suggested that 15-LO-1 plays an important role in angiogenesis and carcinogenesis (Viita et al., 2008). Both angiogenesis and tumor formation in two xenograft models were inhibited in transgenic mice over-expressing 15-LO-1 in ECs (Harats et al., 2005). It has been suggested that several possible pro- versus anti-angiogenesis functions are mediated by metabolites derived from 15-LO-mediated lipid oxidation (Viita et al., 2008). These issues make it difficult to assess the precise contribution of the 15-LO pathway to angiogenesis, atherosclerosis, and tumorigenesis. For example, 15-LO has pro-inflammatory and anti-inflammatory effects in cell cultures and primary cells and opposite effects on atherosclerosis in two different animal species (Wittwer and Hersberger, 2007). There is also substantial evidence for a pro-atherosclerotic effect of 15-LO-1 including its direct contribution to LDL oxidation and to the recruitment of monocytes to the vessel wall (Wittwer and Hersberger, 2007). The explanation to these conflicting observations might reside in the different biological effects of many lipid mediators generated by 15-LO-1

pathway, which have not yet been fully elucidated (Weibel et al., 2009). The present study was designed to elucidate the biosynthesis of 15-oxo-ETE through the actions of 15-LO-1 and 15-PGDH and to explore its potential pharmacological role in angiogenesis, an important mediator of tumorigenesis (Folkman, 2007).

## Materials and Methods

**Materials.** AA (peroxide-free), 15(*S*)-HETE, 15-oxo-ETE, [$^2H_8$]-15(*S*)- HETE, [$^2H_6$]-5-oxo-ETE, CAY10397 were purchased from Cayman Chemical Co. (Ann Arbor, MI). CDC was obtained from BioMol (Plymouth Meeting, PA). CI, diisopropylethylamine, 2,3,4,5,6-pentafluorobenzyl bromide (PFB) bromide and fetal bovine serum (FBS) were purchased from Sigma-Aldrich. Dulbecco's Modified Eagle's Medium (DMEM), RPMI-1640 media, Medium 199 (M199), phosphate buffered saline (PBS), D-glucose, L-glutamine, heparin, penicillin, streptomycin and geneticin were supplied by Invitrogen (Carlsbad, CA). EC growth supplement was purchased from Millipore (Temecula, CA). Recombinant human interleukin (IL)-4 was obtained from BD Biosciences (San Jose, CA). High performance liquid chromatography (LC) grade water, hexane, methanol, and isopropanol were obtained from Fisher Scientific (Fair Lawn, NJ). Gases were supplied by BOC Gases (Lebanon, NJ).

**Mass spectrometry (MS).** The quantitative targeted lipidomics profile was obtained on a triple-quadrupole Finnigan TSQ Quantum Ultra AM mass spectrometer (Thermo Scientific, San Jose, CA) equipped for electron capture negative atmospheric pressure chemical ionization (ECAPCI) (Lee and Blair, 2007; Mesaros et al., 2009). Operating conditions were as follows: spray voltage 4.5 kV, vaporizer temperature at 450 °C and heated capillary temperature was 350

°C with a discharge current of 30 μA applied to the corona needle. A post column addition of 0.75 ml/min of methanol was used to prevent buildup of carbon in the source. Nitrogen was used as the sheath gas and auxiliary gas, set at 60 and 10 (in arbitrary units), respectively. Collision-induced dissociation was performed using argon as the collision gas at 1.5 mTorr in the second (rf-only) quadrupole and the collision energy was set at 18 eV. An additional dc offset voltage was applied to the region of the second multipole ion guide (Q0) at 5 V to impart enough translational kinetic energy to the ions so that solvent adduct ions dissociate to form sample ions. For multiple reaction monitoring (MRM), unit resolution was maintained for both parent and product ions. The following MRM transitions were monitored: 15-HETEs (*m/z* 319 → 219), [$^2H_8$]-15(*S*)-HETE (*m/z* 327 → 226), 15-oxo-ETE (*m/z* 317 → 273) and [$^2H_6$]-5-oxo-ETE (*m/z* 323 → 279).

**LC.** Normal phase chiral LC-ECAPCI/MS analyses were conducted using a Waters Alliance 2690 high performance LC system (Waters Corp., Milford, MA). A Chiralpak AD-H column (250 x 4.6-mm inner diameter, 5 μm; Daicel Chemical Industries, Ltd., West Chester, PA) was employed for gradient 1 with a flow rate of 1.0 ml/min. Solvent A was hexane, and solvent B was methanol/isopropanol (1:1, v/v). Gradient 1 was as follows: 2% B at 0 min, 2% B at 3 min, 3.6% B at 11 min, 8% B at 15 min, 8% B at 27 min, 50% B at 30 min, 50% B at 35 min, 2% B at 37 min and 2% B at 45 min. Separations were performed at 30 °C using a linear gradient.

**Cell Culture.** Murine macrophage RAW 264.7 cells (obtained from American Type Culture Collection, Manassas, VA) were stably transfected with the pcDNA3 plasmid containing the human 15-LO-1 gene (R15L cells) or an empty pcDNA3 plasmid (RMock cells) (Zhu et al., 2008). Cells were cultured in DMEM supplemented with 10% FBS, 4,500 mg/l D-glucose, and 0.5 g/l geneticin. Before the treatment for lipidomics analysis, the culture media was replaced

with serum-free DMEM. HUVECs were a generous gift from Dr. Vladimir Muzykantov (University of Pennsylvania). HUVECs were cultured in Medium 199 supplemented with 10% FBS, 1,000 mg/l L-glutamine, 10,000 mg/l heparin, 15,000 mg/l EC growth supplement, 100,000 units/l penicillin and 100,000 units/l streptomycin. Primary human monocytes were isolated from the peripheral blood of healthy adult donors and purified by the Biomolecular and Cellular Resource Center, Department of Pathology and Laboratory Medicine, University of Pennsylvania in accordance with human subject protocols approved by the Internal Review Board of the National Institutes of Health. Cells were cultured in RPMI 1640 media with 10% FBS, 2 mM L-glutamine, 100,000 units/l penicillin and 100,000 μg/l streptomycin for 2 h. Human IL-4 was added to the cell culture media to reach a final concentration of 1000 pM. Cells were cultured for 40 h at 37 ºC. Before treatment, cell culture media were replaced with serum free RPMI 1640 media containing 2 mM L-glutamine. 50 μM of AA or 5 μM of CI in ethanol was added to the media and cells were incubated for 40 min at 37 ºC. The final concentration of ethanol in the culture media was less than 0.1%. Cells and media were then harvested for further analysis. Cell numbers were counted by a hemocytometer.

**AA or CI Treatment of Primary Human Monocytes.** Primary human monocytes were cultured as described above. The media was removed and replaced with serum-free RPMI-1640 media containing 2 mM L-glutamine. AA (50 μM final concentration) or CI (5 μM final concentration) was added to the media. Cells were then incubated for 40 min at 37 $^{o}$C. A portion of cell supernatant (3 ml) was transferred into a glass tube and adjusted to pH 3 with 2.5 N hydrochloric acid. Lipids were extracted with diethyl ether (4 ml x 2) and the organic layer was then evaporated to dryness under nitrogen. 100 μl of acetonitrile, 100 μl of PFB bromide in acetonitrile (1:19, v/v) and 100 μl of diisopropylethylamine in acetonitrile (1:9, v/v) were added

to the residue and the solution was heated at 60 $^{o}$C for 60 min. The solution was allowed to cool down, evaporated to dryness under nitrogen at room temperature, dissolved in 100 µl of hexane/ethanol (97:3, v/v) and an aliquot of 20 µl was used for normal-phase chiral LC-ECAPCI/MRM/MS analysis using gradient 1 as described above.

**AA treatment of R15L and RMock Cells.** R15L cells and RMock cells were cultured in DMEM supplemented with 10% FBS, 4,500 mg/l D-glucose, and 0.5 g/l geneticin. The media was removed and replaced with serum-free DMEM containing peroxide-free AA (10 µM final concentration). Cells were then incubated for 0 min, 1 min, 5 min, 10 min, 30 min, 40 min, 1 h, 2 h, 3 h and 24 h at 37 $^{o}$C. After each incubation, a portion of cell supernatant (3 ml) was transferred into a glass tube and cell numbers were counted by a hemocytometer. Blank media standards (3 ml) were prepared, spiked with the following amounts of authentic lipid standards [15(*R*,*S*)-HETEs, 15-oxo-ETE]: 10, 20, 50, 100, 200, 500 and 1000 pg. A mixture of internal standards [$^{2}H_{8}$]-15(*S*)-HETE, [$^{2}H_{6}$]-5-oxo-ETE, 1 ng each was added to each cell supernatant sample and standard solution. The samples and standards were adjusted to pH 3 with 2.5 N hydrochloric acid. Extraction of 15(*R S*)-HETEs and 15-oxo-ETE from cell culture media and LC-ECAPCI/MRM/MS analyses were performed as described above. Calibration curves were obtained with linear regressions of analyte versus internal standard peak-area ratio 15(*R,S*)-HETEs/[$^{2}H_{8}$]-15(*S*)-HETE, 15-oxo-ETE/[$^{2}H_{6}$]-5-oxo-ETE against analyte concentrations. Concentrations of 15(*R,S*)-HETEs and 15-oxo-ETE in the media supernatants were calculated by interpolation from the calculated regression lines.

**CI Treatment of R15L Cells.** R15L cells were cultured as described above. The media was removed and replaced with serum-free DMEM containing CI (5 µM final concentration). Cells were then incubated for 0 min, 1 min, 5 min, 10 min, 30 min, 40 min, 1 h, 2 h, 3 h and 24 h at 37

Molecular Pharmacology Fast Forward. Published on June 17, 2009 as DOI: 10.1124/mol.109.057489
This article has not been copyedited and formatted. The final version may differ from this version.



$^{o}$C. Extraction and quantitation of 15(*R,S*)-HETEs and 15-oxo-ETE from cell culture media (3 ml) were performed as described above.

**AA or CI Treatment of R15L Cells with LO inhibitor CDC.** R15L cells were cultured as described above. Cells were treated with either 10 μM AA for 10 min or 5 μM CI for 40 min with or without the pretreatment with 20 μM CDC for 40 min. Extraction and quantitation of 15-oxo-ETE from cell culture media (3 ml) were performed as described above.

**15(*S*)-HETE or AA Treatment of R15L Cells with 15-PGDH inhibitor CAY10397.** R15L cells were cultured as described above until almost confluent. The media was removed and replaced with serum-free DMEM containing various doses of CAY10397 (0 μM, 5 μM, 10 μM, 15 μM, 25 μM, 50 μM, and 100 μM final concentration). Cells were then incubated for 4 h at 37 $^{o}$C followed by incubation with additional 15(*S*)-HETE (50 nM final concentration) or AA (10 μM final concentration) for 10 min. Extraction and quantitation of 15(*S*)-HETE and 15-oxo-ETE from cell culture media (3 ml) were performed as described above. $IC_{50}$ and $EC_{50}$ values for CAY10397 were calculated from the equation of the non-linear regression dose-response curves assuming that the 15(*S*)-HETE bound to the enzyme following the laws of mass action.

**Cell Proliferation 5-bromo-2-deoxyuridine (BrdU) Assay.** Equal numbers (1000 cells/well) of HUVECs were plated as described above in 24-well plates and allowed to attach overnight. Cells were then treated with 15-oxo-ETE dissolved in ethanol (0 μM, 1 μM, 5 μM, 10 μM or 20 μM final concentrations). The final concentration of ethanol in the culture media was less than 0.1%. Cell proliferation was assessed for two days by a commercially available BrdU assay kit according to the manufacturer's protocol [Roche® Cell Proliferation Enzyme-linked immunosorbent assay (ELISA) BrdU (colorimetric)]. The absorbance at λ = 370 nm

obtained from the assay was normalized to the cell numbers according to a standard curve. Each data point represents the mean value from triplicate wells.

**Extraction of Intracellular Eicosanoids in HUVECs after Incubation with 15-oxo-ETE.** HUVECs were cultured as described above. The media was removed and replaced with the media containing 1 μM or 10 μM 15-oxo-ETE. Cells were then incubated for 30 min, 1 h, 4 h, 24 h and 48 h at 37 $^{o}$C. After each incubation, cells were washed with PBS and re-suspended in 1 ml PBS. Blank PBS (1 ml) solutions were prepared, spiked with the following amounts of authentic lipid standards [15(*R*,*S*)-HETEs, 15-oxo-ETE]: 10, 20, 50, 100, 200, 500 and 1000 pg. A mixture of internal standards [$^{2}H_{8}$]-15(*S*)-HETE, [$^{2}H_{6}$]-5-oxo-ETE, 1ng each was added to each analytical sample and standard solution. Lipids were extracted with chloroform/methanol (2:1, v/v, 5 ml x 2). The organic layer was then washed with 0.9% sodium chloride (1 ml x 2) and evaporated to dryness under nitrogen. Lipid samples were further derivatized with PFB bromide, reconstituted in hexane/ethanol and analyzed by LC-ECAPCI/MRM/MS as described above.

## Results

**AA- or CI-mediated Production of 15(*R*,*S*)-HETEs and 15-oxo-ETE in Primary Human Monocytes.** The cytokine IL-4 induces 15-LO-1 expression in human monocytes. Primary human monocytes were incubated with AA (50 μM) or CI (5 μM) for 40 min following 40 h pretreatment with IL-4 (1 nM). Compared to the non-treated IL-4 induced monocytes, the chromatograms from LC-ECAPCI/MRM/MS analyses demonstrated the formation of 15(*S*)-HETE [retention time (rt), 15.5 min] in IL-4-induced primary human monocytes treated with

exogenous AA or CI (Fig. 2A). There was very little 15(*R*)-HETE (rt, 15.4 min) compared with 15(*S*)-HETE (Fig. 2A). 15-oxo-ETE was also identified (rt, 8.10 min) in IL-4-induced primary human monocytes with either AA or CI treatment (Fig. 2B). The signal intensity of 15-oxo-ETE was approximately 3-fold lower ($1.34 \times 10^7$) than the intensity of 15(*S*)-HETE ($4.35 \times 10^7$) in AA-treated cells and approximately 10-fold lower ($5.04 \times 10^5$) than the intensity of 15(*S*)-HETE ($4.05 \times 10^6$) in CI-treated cells (Figs. 2A and 2B).

**AA-mediated Production of 15(*R,S*)-HETEs and 15-oxo-ETE in R15L Cells.** R15L cells and RMock cells were incubated with 10 μM AA for a time-course of 24 h. LC-ECAPCI/MRM/MS analyses of the R15L cell supernatants demonstrated the production of 15-oxo-ETE (rt, 8.67 min) and 15(*S*)-HETE (rt, 16.15 min) within 5 min treatment of AA (Fig. 3A). Extracted chromatograms for 15-oxo-ETE, [$^2H_6$]-5-oxo-ETE, 15(*R*)-HETE, 15(*S*)-HETE and [$^2H_8$]-15(*S*)-HETE are shown in Fig. 3A. [$^2H_6$]-5-oxo-ETE and [$^2H_8$]-15(*S*)-HETE were used as internal standards to quantify 15-oxo-ETE and 15(*R,S*)-HETEs, respectively. Fig. 3B displays the production of 15(*R*)- and 15(*S*)-HETE by R15L and RMock cells upon AA treatment. 15(*S*)-HETE was the predominant eicosanoid isomer released by R15L cells, with negligible amounts of 15(*R*)-HETE produced in response to AA treatment. Furthermore, 15(*S*)-HETE level peaked within 5 min treatment of AA (500 pmol/$10^6$ cells) (Fig. 3B). In contrast, both 15(*R*)- and 15(*S*)-HETE production in RMock cells were close to limit of detection (Fig. 3B). The time course of 15-oxo-ETE produced in R15L cells upon AA treatment is similar to that of 15(*S*)-HETE with maximum level of 15-oxo-ETE observed (120 pmol/$10^6$ cells) within 5 min of AA treatment, then continuing to diminish over the remainder of the 24 h treatment period (Fig. 3C). Again, there was very little production of 15-oxo-ETE in RMock cells (Fig. 3C).

**CI-mediated Production of 15(*R*,*S*)-HETEs and 15-oxo-ETE in R15L Cells.** CI increases the intracellular calcium concentration, which recruits 15-LO from the cytosol to the inner side of the plasma membrane, oxidizes AA to 15(*S*)-HPETE, which is subsequently reduced and released as 15(*S*)-HETE. The chromatograms of LC-ECAPCI/MRM/MS analyses demonstrated the production of the endogenous 15-oxo-ETE (rt, 8.31 min) and 15(*S*)-HETE (rt, 15.93 min) after 40 min treatment of 5 μM CI (Fig. 4A). Maximum synthesis of 15(*S*)-HETE was observed at 18 pmol/$10^6$ cells within 1 h of the CI treatment, and decreased to limit of detection after 3 h, while there was very little production of 15(*R*)-HETE (rt, 12.60 min) throughout the time course of the treatment (Fig. 4B). Similarly, 15-oxo-ETE production peaked at 2 pmol/$10^6$ cells after 40 min of the CI treatment, and declined to limit of detection after 3 h (Fig. 4C).

**Effect of CDC on 15-oxo-ETE Production in R15L Cells**. CDC is a LO inhibitor that inhibits the production of 15-LO-mediated lipid metabolites (Cho et al., 1991). R15L cells were treated with 10 μM AA for 10 min or 5 μM CI for 40 min, with or without 40 min pretreatment with 20 μM CDC. AA treatment alone of R15L cells led to the production of 15-oxo-ETE (40 pmol/$10^6$ cells) as well as 15(*S*)-HETE (420 pmol/$10^6$ cells) (Fig. 5A and 5C, respectively). Pretreatment with CDC resulted in significant inhibition of 15-oxo-ETE production by almost 70% (12 pmol/$10^6$ cells), and 15(*S*)-HETE production by almost 95% (20 pmol/$10^6$ cells) (Figs. 5A and 5C. respectively). CDC treatment by itself did not lead to 15-oxo-ETE or 15(*S*)-HETE generation (Figs. 5A and 5C respectively). CI treatment generated 2 pmol/$10^6$ cells of 15-oxo-ETE (Fig. 5B) and 35 pmol/$10^6$ cells of 15(*S*)-HETE (Fig. 5D) in R15L cells. CDC pretreatment completely abolished both the CI-mediated 15-oxo-ETE and 15(*S*)-HETE production (Figs. 5B and 5D, respectively). CDC treatment alone had no effect on 15-oxo-ETE or 15(*S*)-HETE

Molecular Pharmacology Fast Forward. Published on June 17, 2009 as DOI: 10.1124/mol.109.057489
This article has not been copyedited and formatted. The final version may differ from this version.



generation (Figs. 5B and 5D, respectively). These data further confirmed that both 15(*S*)-HETE and 15-oxo-ETE were 15-LO-derived metabolites of endogenous AA.

**Kinetics of 15(S)-HETE Metabolism to 15-oxo-ETE by R15L Cells.** To study the kinetics of 15(*S*)-HETE metabolism in R15L cells, R15L cells were incubated with 15(*S*)-HETE (0.9 μM) for 3 h. The level of 15(*S*)-HETE in the cell media declined from 0.9 μM to being close to the limit of detection in 3 h (Fig. 6A). The half-life of 15(*S*)-HETE was determined to be 21 min and the pseudo first-order rate constant (k) was 0.0331 $min^{-1}$ (Fig. 6B). Concomitantly, the level of 15-oxo-ETE in the cell media was observed to peak within 5 min of 15(*S*)-HETE treatment with the concentration of 0.022 (± 0.002) μM, and declined to being close to the limit of detection in 3 h (Fig. 6C). The half-life of 15-oxo-ETE was determined to be 11 min and the pseudo first-order rate constant (k) was 0.0643 $min^{-1}$ (Fig. 6D).

**Effect of CAY10397 on 15-oxo-ETE and 15(S)-HETE in R15L cells.** CAY10397 is a selective inhibitor of the 15-PGDH that oxidizes 15-hydroxyl group of prostaglandins (PGs) to a 15-oxo-group (Berry et al., 1983; Quidville et al., 2006). To determine the effect of CAY10397 on AA-derived 15(*S*)-HETE and 15-oxo-ETE, R15L cells were treated with 10 μM AA for 10 min, with or without the pretreatment with various doses of CAY10397 (0-100 μM) for 4 h. This resulted in a significant inhibition of the production of 15-oxo-ETE (Fig. 7A) and a simultaneous accumulation of 15(*S*)-HETE in a dose-dependent manner (Fig. 7B). To confirm that 15-PGDH was the enzyme that oxidized 15(*S*)-HETE to 15-oxo-ETE, R15L cells were treated with 50 nM 15(*S*)-HETE for 10 min, with or without the pretreatment with various doses of CAY10397 (0-100 μM) for 4 h. 15(*S*)-HETE treatment alone gave rise to the production of 15-oxo-ETE (3 pmol/$10^6$ cells). CAY10397 pretreatment resulted in dose dependent inhibition of 15-oxo-ETE production. The inhibition reached 80% in the presence of 100 μM CAY10397 (Fig. 7C).

Molecular Pharmacology Fast Forward. Published on June 17, 2009 as DOI: 10.1124/mol.109.057489
This article has not been copyedited and formatted. The final version may differ from this version.



CAY10397 also caused a concomitant dose-dependent increase in 15(*S*)-HETE concentrations after the addition of exogenous 15(*S*)-HETE (Fig. 7D). CAY10397 treatment by itself in the absence of AA did not lead to 15-oxo-ETE generation (data not shown). The $IC_{50}$ of CAY10397 on AA-mediated (Fig. 7A) or 15(*S*)-HETE-mediated (Fig. 7C) 15-oxo-ETE production were very similar at 17.3 μM and 13.2 μM, respectively. The Hill coefficient for the inhibition of 15(*S*)-HETE-derived 15-oxo-ETE was -1.2 indicating that the 15(S)-HETE and CAY10397 were binding at the same site (Fig. 7C). However, a Hill coefficient of -2.2 was obtained for the inhibition of AA-derived 15-oxo-ETE indicating that there was cooperativity in the inhibition of these more complex ligand/binding site interactions (Fig. 7A). The $EC_{50}$ for CAY10397-induced increase in AA-mediated 15(*S*)-HETE formation was 19.6 μM (Fig. 7B), which was similar to the $IC_{50}$ of 17.3 μM for inhibition of AA-mediated 15-oxo-ETE formation (Fig. 7A). As expected, the Hill coefficient (-3.0) deviated from -1.0 because of cooperativity effects. The effect of CAY10397 on 15(*S*)-HETE concentrations after the addition of exogenous 15(*S*)-HETE was too complex to analyze using conventional non-linear binding models (Fig. 7D).

**Effect of 15-oxo-ETE on Proliferation of HUVECs.** In order to examine the effect of 15-oxo-ETE on cell proliferation, colorimetric BrdU ELISA assays were performed on HUVECs treated with different concentrations (1-20 μM) of 15-oxo-ETE for a 48 h period. BrdU incorporation was analyzed and the corresponding cell number was determined from a standard curve. DNA synthesis in the HUVECs (as measured by BrdU incorporation) was inhibited by 15-oxo-ETE. This resulted in a dose-dependent decrease in cellular proliferation as reflected by the cell count determined from the BrdU standard curve (Fig. 8A).

**15-oxo-ETE uptake into HUVECs.** Cells were incubated with 1 μM or 10 μM of 15-oxo-ETE for 48 h. For 1 μM 15-oxo-ETE incubation, the intracellular concentrations of 15-oxo-ETE

were measured during the time course. The intracellular concentrations of 15-oxo-ETE increased from below the limit of detection at 0 min to 408.08 (± 12.13) nM at 30 min, 154.18 (± 14.91) nM at 1 h, 70.18 (± 9.85) nM at 4 h and below the limit of detection after 24 h (Fig. 8B). In HUVECs incubated with 10 μM of 15-oxo-ETE, the intracellular concentrations of 15-oxo-ETE were measured at 3.19 (± 1.10) μM at 30 min, 2.48 (± 0.21) μM at 1 h, 2.42 (± 0.52) μM at 4 h and below the limit of detection after 24 h (Fig. 8C).

## Discussion

IL-4 stimulated human monocytes were found to secrete primarily 15(S)-HETE and15-oxo-ETE when treated with exogenous AA or with CI (Fig. 2). Brinckmann *et al*. reported that 15-LO-1 translocated to plasma membrane in a calcium-dependent manner in rabbit hematopoietic cells and that the translocation activated the oxygenase activity of the enzyme (Brinckmann et al., 1998). It is known that 15-LO-1 has a broad substrate specificity so that it can oxidize esterified lipids as well as protein-lipid assemblies (Kühn and O'Donnell, 2006). Furthermore, Maskrey *et al*. showed that when IL-4-treated monocytes were stimulated with CI, they generated predominantly esterified 15-HETE; with many fold less free 15-HETE (Maskrey et al., 2007). These studies suggest that CI treatment of the monocytes resulted in translocation of 15-LO-1 to the plasma membrane so that it was no longer present the cytosol. 15(*S*)-HPETE was then formed primarily on esterified AA rather than from free of AA released by CI-mediated translocation of cytosolic phospholipase $A_2$ ($cPLA_2$) to the membrane. The resulting esterified 15(*S*)-HPETE was then reduced to 15(*S*)-HETE (Schnurr et al., 1999) and a significant amount then released by $cPLA_2$-mediated hydrolysis of the esterified 15(*S*)-HETE and released from the

cells as suggested previously by Chaitidis *et al*. (Chaitidis et al., 1998). Indeed, CI treatment of R15L cells led to the production of 15(*S*)-HETE and 15-oxo-ETE (Fig. 2), confirming that they are metabolites of endogenously-derived AA. These data also suggest that 15(*S*)-HETE is the predominant precursor of 15-oxo-ETE in 15-LO-1 mediated metabolism of endogenously-derived AA. This contrasts with COX-2-mediated formation of 15-oxo-ETE, which could be derived from 15(*S*)-HPETE, 15(*S*)-HETE, or the corresponding 15(*R*)-enantiomers (Lee et al., 2007).

A targeted quantitative chiral lipidomics analysis showed that 15(*S*)-HETE and 15-oxo-ETE were also major metabolites derived from exogenous and endogenous AA in R15L cells (Figs. 3 and 4). Moreover, the RMock cells that do not express any human 15-LO-1 failed to generate these metabolites (Figs. 3 and 4). Pre-treatment of R15L cells with CDC, a LO inhibitor, led to a significant reduction in 15-oxo-ETE and 15(*S*)-HETE levels that were produced by AA treatment alone (Fig. 5A and 5C respectively). CDC pre-treatment also led to complete inhibition of 15-oxo-ETE and 15(*S*)-HETE production by CI treatment in R15L cells (Fig. 5B and 5D respectively). CDC treatment by itself did not generate any 15(*S*)-HETE and 15-oxo-ETE in R15L cells. Thus, these data provide further evidence that 15(*S*)-HETE and 15-oxo-ETE are 15-LO-specific metabolites of AA. 15(*S*)-HETE was found to be rapidly converted into 15-oxo-ETE, with approximately 90% conversion occurring within 3 h in the R15L cells (Fig. 6A). A kinetic plot (Fig. 6B) revealed that the half-life of 15(*S*)-HETE in R15L cells was 21 min with a pseudo first-order rate constant of 0.0331 $min^{-1}$. These data are consistent with findings from a similar study involving COX-2 expressing RIES cells (Lee et al., 2007).

15-PGDH catalyzes $NAD^+$-mediated oxidation of 15(*S*)-hydroxyl group of PGs and lipoxins (Quidville et al., 2006; Tai et al., 2007). It is a key PG catabolism enzyme, converting (for

example) $PGF_{2\alpha}$ to 15-oxo-$PGF_{2\alpha}$ (Fig. 1). Our previous studies had established 15-oxo-ETE as a downstream metabolite of 15(*S*)-HETE (Lee et al., 2007); however, the enzyme responsible for this oxidation was not identified. In the present study we have shown that the specific 15-PGDH inhibitor (CAY10397) significantly decreased the production of 15-oxo-ETE and the metabolism of 15(*S*)-HETE in the macrophages treated with either AA (Fig. 7A) or 15(*S*)-HETE (Fig. 7C). The $IC_{50}$ values for CAY10397-mediated 15-oxo-ETE inhibition were determined to be 17.3 and 13.2 μM, respectively. There was a concomitant increase in 15(*S*)-HETE concentrations after inhibition of AA- (Fig. 7B) and 15(*S*)-HETE-mediated (Fig. 7D) 15-oxo-ETE formation. These data clearly show that 15-oxo-ETE arose through the oxidation of 15(*S*)-HETE by murine 15-PGDH. Mouse 12/15 LO, which is the counterpart of human 15-LO-1, produces both 12-LO- and 15-LO-derived lipid metabolites (Kühn and O'Donnell, 2006; Middleton et al., 2006). Thus, it is not clear that the phenotypes in 12/15-LO-deficient mice are due to lack of 12-LO- or 15-LO-derived lipid mediators. In this regard, the mouse R15L macrophage cell line, which expresses human 15-LO-1, provided an excellent model to identify 15-LO-derived lipid metabolites.

15-oxo-ETE was rapidly cleared from the R15L cells, with a half-life of only 11 min, indicating that it underwent further metabolism (Fig. 6D). We showed previously that 15-oxo-ETE forms a GSH-adduct through GSH *S*-transferase-mediated Michael addition (Lee et al., 2007). Other studies have shown that AA-derived metabolites such as leukotriene $C_4$ and 5-oxo-ETE can also form GSH-adducts (Murphy and Zarini, 2002; Blair, 2006). This suggests that 15-oxo-ETE is also metabolized to a GSH-adduct in the R15L cells, which would account for its rapid clearance.

A previous study reported that 15-oxo-ETE has very low but detectable chemotactic activity in human monocytes *in vitro* (Sozzani et al., 1996). Another study reported that 15-oxo-ETE can inhibit proliferation in breast cancer cell lines, however, only at concentrations exceeding 100 μM (O'Flaherty et al., 2005). The present study has shown that 15-oxo-ETE inhibits BrdU incorporation and HUVEC proliferation in a time-dependent manner at much lower concentrations (down to 1 μM) than reported for breast cancer cells (Fig. 8A). Rapid 15-oxo-ETE uptake in R15L cells was quantified in order to confirm that this pharmacological effect was in fact due to the presence of intracellular 15-oxo-ETE. Rapid uptake was observed at extra-cellular concentrations of 1 μM (Fig. 8B) and 10 μM (Fig. 8C) showing that 15-oxo-ETE can readily cross the plasma membrane.

The 15-oxo-ETE analogs, 5-oxo-ETE and 15d-$PGJ_2$, (15-deoxy-$\Delta^{12,14}$-prostaglandin $J_2$, Fig. 1) modulate cell proliferation and apoptosis as peroxisome proliferator-activated receptor (PPAR)γ agonists (O'Flaherty et al., 2005). PPARγ agonists inhibit experimental models of atherosclerosis and the formation of macrophage foam cells (Li et al., 2004). It has been proposed that 15d-$PGJ_2$ inhibits proliferation by covalently binding to the thiol residues in IκB kinase or p50 subunit of NF-κB through a Michael addition reaction to block the proteins from performing their survival function, using a PPARγ independent mechanism (Cernuda-Morollón et al., 2001). The similar structural features present in 5-oxo-ETE, 15d-$PGJ_2$ and 15-oxo-ETE (Fig. 1) suggest that 15-oxo-ETE might also modulate cell proliferation and apoptosis through PPARγ-dependent and/or PPARγ-independent mechanism.

Our observation that 15-oxo-ETE can inhibit HUVEC proliferation provides a novel mechanism that could promote endothelial dysfunction (Carmeliet, 2005). It is interesting to note that 15-PGDH is down-regulated *in vivo* in colorectal cancer (Backlund et al., 2005). In

view of our new findings, it is intriguing to speculate that down-regulation of 15-PGDH inhibits the production of 15-oxo-ETE and suppresses the anti-proliferative effect of 15-oxo-ETE on ECs, thus potentially exacerbating colorectal cancer. Moreover, the capability of 15-oxo-ETE to inhibit EC proliferation suggests that it might be involved in other conditions where macrophage and/or endothelial cell dysfunction play a role such as in chronic inflammation, atherosclerosis, leukemia, and asthma. Chronic inflammation is known to be involved as a critical component in angiogenesis as well as cancer (Fierro et al., 2002). Therefore, depending on the location and the local environment *in vivo*, reduction of EC proliferation and migration in response to 15-oxo-ETE treatment might also be responsible for anti-inflammatory activity. Previous studies have demonstrated that overexpression of 15-LO-1 is associated with an anti-inflammatory response in both rabbit and murine models (Merched et al., 2008). Furthermore, aspirin-triggered 15-LO-1 metabolites of AA (lipoxins) have an anti-inflammatory activity through inhibition of EC proliferation (Fierro et al., 2002, Serhan et al., 2008). Lipoxins have also been shown to promote resolution, a process known to involve active biochemical programs that enables inflamed tissues to return to homeostasis (Serhan et al., 2008). 15-LO-1 activation during the process of inflammation has also been correlated with switching the metabolism of AA and other ω-3 polyunsaturated fatty acids to produce pro-resolving lipid mediators such as resolvins and protectins. Taken together, 15-LO-1 up-regulation can result in the production of anti-inflammatory as well as pro-resolving activities (Serhan et al., 2008). Localized formation of 15-oxo-ETE production *in vivo* could be involved in both of these processes.

In summary, our studies have provided additional insight into IL-4-induced 15-LO-1 signaling in monocyte/macrophages and potential cell-cell interactions (Fig. 9). After IL-4 binds to its receptor, 15-LO-1 expression is induced via Janus kinase 1 (JAK1) activation, followed by

Molecular Pharmacology Fast Forward. Published on June 17, 2009 as DOI: 10.1124/mol.109.057489
This article has not been copyedited and formatted. The final version may differ from this version.



dimerization and nuclear trans-localization of signal transducer and activator of transcription 6 (Stat6) (Chatila, 2004). With elevated intracellular calcium concentrations, 15-LO-1 is recruited to the inner side of the plasma membrane where it converts esterified AA to 15(*S*)-HPETE. Esterified 15(*S*)-HPETE is reduced to 15(*S*)-HETE and released as the free acid by c-$PLA_2$. The 15(*S*)-HETE is then oxidized to 15-oxo-ETE by 15-PGDH, and 15-oxo-ETE is conjugated to form a 15-oxo-ETE-GSH-adduct (OEG), which is then hydrolyzed by γ-glutamyltranspeptidase (GGTP) to a 15-oxo-ETE-cysteinyl-adduct (OEC) (Figure 9) (Lee et al., 2007). Released 15-oxo-ETE can inhibit EC proliferation which could further prevent EC growth and that in turn could lead to the inhibition of angiogenesis. In the absence of 15-PGDH (Backlund et al., 2005), no 15-oxo-ETE would be formed and therefore the anti-angiogenesis activity on ECs would be lost. This could then lead to increased tumor growth and metastasis. Therefore, these studies provide a pharmacological basis for the design of new targeted therapeutic strategies to inhibit angiogenesis.

**Acknowledgement**

We thank Dr. Colin D. Funk (Queen's University, Kingston, ON, Canada) for kind gifts of the pcDNA3 plasmid containing the human 15-LOX-1 gene and the empty pcDNA3 plasmid.

## References

Backlund MG, Mann JR, Holla VR, Buchanan FG, Tai HH, Musiek ES, Milne GL, Katkuri S, and Dubois RN (2005) 15-Hydroxyprostaglandin Dehydrogenase Is Down-Regulated in Colorectal Cancer. *J Biol Chem* **280**:3217-3223.

Bergholte JM, Soberman RJ, Hayes R, Murphy RC, and Okita RT (1987) Oxidation of 15-Hydroxyeicosatetraenoic Acid and Other Hydroxy Fatty Acids by Lung Prostaglandin Dehydrogenase. *Arch Biochem Biophys* **257**:444-450.

Berry CN, Hoult JR, Peers SH, and Agback H (1983) Inhibition of Prostaglandin 15-Hydroxydehydrogenase by Sulphasalazine and a Novel Series of Potent Analogues. *Biochem Pharmacol* **32**:2863-2871.

Blair IA (2006) Endogenous Glutathione Adducts. *Curr Drug Metab* **7**:853-872.

Blair IA (2008) DNA-Adducts With Lipid Peroxidation Products. *J Biol Chem* **283**:15545-15549.

Brinckmann R, Schnurr K, Heydeck D, Rosenbach T, Kolde G, and Kühn H (1998) Membrane Translocation of 15-Lipoxygenase in Hematopoietic Cells Is Calcium-Dependent and Activates the Oxygenase Activity of the Enzyme. *Blood* **91**:64-74.

Bryant RW, Bailey JM, Schewe T, and Rapoport SM (1982) Positional Specificity of a Reticulocyte Lipoxygenase. Conversion of Arachidonic Acid to 15-S-Hydroperoxy-Eicosatetraenoic Acid. *J Biol Chem* **257**:6050-6055.

Carmeliet P (2005) Angiogenesis in Life, Disease and Medicine. *Nature* **438**:932-936.

Cernuda-Morollón E, Pineda-Molina E, Cañada FJ, and Pérez-Sala D (2001) 15-Deoxy-Delta 12,14-Prostaglandin J2 Inhibition of NF-KappaB-DNA Binding Through Covalent Modification of the P50 Subunit. *J Biol Chem* **276**:35530-35536.

Cha YI, Solnica-Krezel L, and Dubois RN (2006) Fishing for Prostanoids: Deciphering the Developmental Functions of Cyclooxygenase-Derived Prostaglandins. *Dev Biol* **289**:263-272.

Chaitidis P, Schewe T, Sutherland M, Kühn H, and Nigam S (1998) 15-Lipoxygenation of Phospholipids May Precede the Sn-2 Cleavage by Phospholipases A2: Reaction Specificities of Secretory and Cytosolic Phospholipases A2 Towards Native and 15-Lipoxygenated Arachidonoyl Phospholipids. *FEBS Lett* **434**:437-441.

Chatila TA (2004) Interleukin-4 Receptor Signaling Pathways in Asthma Pathogenesis. *Trends Mol Med* **10**:493-499.

Cho H, Ueda M, Tamaoka M, Hamaguchi M, Aisaka K, Kiso Y, Inoue T, Ogino R, Tatsuoka T, Ishihara T, and . (1991) Novel Caffeic Acid Derivatives: Extremely Potent Inhibitors of 12-Lipoxygenase. *J Med Chem* **34**:1503-1505.

Fierro IM, Kutok JL, and Serhan CN (2002) Novel Lipid Mediator Regulators of Endothelial Cell Proliferation and Migration: Aspirin-Triggered-15R-Lipoxin A(4) and Lipoxin A(4). *J Pharmacol Exp Ther* **300**:385-392.

Folkman J (2007) Angiogenesis: an Organizing Principle for Drug Discovery? *Nat Rev Drug Discov* **6**:273-286.

Gonzalez-Periz A and Claria J (2007) New Approaches to the Modulation of the Cyclooxygenase-2 and 5-Lipoxygenase Pathways. *Curr Top Med Chem* **7**:297-309.

Gulliksson M, Brunnstrom A, Johannesson M, Backman L, Nilsson G, Harvima I, Dahlen B, Kumlin M, and Claesson HE (2007) Expression of 15-Lipoxygenase Type-1 in Human Mast Cells. *Biochim Biophys Acta* **1771**:1156-1165.

Harats D, Ben-Shushan D, Cohen H, Gonen A, Barshack I, Goldberg I, Greenberger S, Hodish I, Harari A, Varda-Bloom N, Levanon K, Grossman E, Chaitidis P, Kühn H, and Shaish A

(2005) Inhibition of Carcinogenesis in Transgenic Mouse Models Over-Expressing 15-Lipoxygenase in the Vascular Wall Under the Control of Murine Preproendothelin-1 Promoter. *Cancer Lett* **229**:127-134.

Huo Y, Zhao L, Hyman MC, Shashkin P, Harry BL, Burcin T, Forlow SB, Stark MA, Smith DF, Clarke S, Srinivasan S, Hedrick CC, Praticó D, Witztum JL, Nadler JL, Funk CD, and Ley K (2004) Critical Role of Macrophage 12/15-Lipoxygenase for Atherosclerosis in Apolipoprotein E-Deficient Mice. *Circulation* **110**:2024-2031.

Jian W, Lee SH, Williams MV, and Blair IA (2009) 5-Lipoxygenase-Mediated Endogenous DNA Damage. *J Biol Chem*April 24. [Epub ahead of print]; doi/10.1074/jbc.M109.011841.

Kühn H and Borchert A (2002) Regulation of Enzymatic Lipid Peroxidation: the Interplay of Peroxidizing and Peroxide Reducing Enzymes. *Free Radic Biol Med* **33**:154-172.

Kühn H and Chan L (1997) The Role of 15-Lipoxygenase in Atherogenesis: Pro- and Antiatherogenic Actions. *Curr Opin Lipidol* **8**:111-117.

Kühn H and O'Donnell VB (2006) Inflammation and Immune Regulation by 12/15-Lipoxygenases. *Prog Lipid Res* **45**:334-356.

Lee SH and Blair IA (2007) Targeted Chiral Lipidomics Analysis by Liquid Chromatography Electron Capture Atmospheric Pressure Chemical Ionization Mass Spectrometry (LC-ECAPCI/MS). *Methods Enzymol* **453**:159-174.

Lee SH, Rangiah K, Williams MV, Wehr AY, Dubois RN, and Blair IA (2007) Cyclooxygenase-2-Mediated Metabolism of Arachidonic Acid to 15-Oxo-Eicosatetraenoic Acid by Rat Intestinal Epithelial Cells. *Chem Res Toxicol* **20**:665-1675.

Li AC, Binder CJ, Gutierrez A, Brown KK, Plotkin CR, Pattison JW, Valledor AF, Davis RA, Willson TM, Witztum JL, Palinski W, and Glass CK (2004) Differential Inhibition of

Macrophage Foam-Cell Formation and Atherosclerosis in Mice by PPARalpha, Beta/Delta, and Gamma. *J Clin Invest* **114**:1564-1576.

Maskrey BH, Bermudez-Fajardo A, Morgan AH, Stewart-Jones E, Dioszeghy V, Taylor GW, Baker PR, Coles B, Coffey MJ, Kuhn H, and O'Donnell VB (2007) Activated Platelets and Monocytes Generate Four Hydroxyphosphatidylethanolamines Via Lipoxygenase. *J Biol Chem* **282**:20151-20163.

Merched AJ, Ko K, Gotlinger KH, Serhan CN, and Chan L (2008) Atherosclerosis: Evidence for Impairment of Resolution of Vascular Inflammation Governed by Specific Lipid Mediators. *FASEB J* **22**:3595-3606.

Mesaros C, Lee SH, and Blair IA (2009) Targeted Quantitative Analysis of Eicosanoid Lipids in Biological Samples Using Liquid Chromatography-Tandem Mass Spectrometry. *J Chromatogr B* Mar 25 [Epub ahead of print]; DOI:10.1016/j.jchromb.2009.03.011.

Middleton MK, Zukas AM, Rubinstein T, Jacob M, Zhu P, Zhao L, Blair I, and Pure E (2006) Identification of 12/15-Lipoxygenase As a Suppressor of Myeloproliferative Disease. *J Exp Med* **203**:2529-2540.

Murphy RC and Zarini S (2002) Glutathione Adducts of Oxyeicosanoids. *Prostaglandins Other Lipid Mediat* **68-69**:471-482.

O'Flaherty JT, Rogers LC, Paumi CM, Hantgan RR, Thomas LR, Clay CE, High K, Chen YQ, Willingham MC, Smitherman PK, Kute TE, Rao A, Cramer SD, and Morrow CS (2005) 5-Oxo-ETE Analogs and the Proliferation of Cancer Cells. *Biochim Biophys Acta* **1736**:228-236.

Porter NA, Caldwell SE, and Mills KA (1995) Mechanisms of Free Radical Oxidation of Unsaturated Lipids. *Lipids* **30**:277-290.

Powell WS and Rokach J (2005) Biochemistry, Biology and Chemistry of the 5-Lipoxygenase Product 5-Oxo-ETE. *Prog Lipid Res* **44**:154-183.

Quidville V, Segond N, Lausson S, Frenkian M, Cohen R, and Jullienne A (2006) 15-Hydroxyprostaglandin-Dehydrogenase Is Involved in Anti-Proliferative Effect of Non-Steroidal Anti-Inflammatory Drugs COX-1 Inhibitors on a Human Medullary Thyroid Carcinoma Cell Line. *Prostaglandins Other Lipid Mediat* **81**:14-30.

Salomon RG, Kaur K, Podrez E, Hoff HF, Krushinsky AV, and Sayre LM (2000) HNE-Derived 2-Pentylpyrroles Are Generated During Oxidation of LDL, Are More Prevalent in Blood Plasma From Patients With Renal Disease or Atherosclerosis, and Are Present in Atherosclerotic Plaques. *Chem Res Toxicol* **13**:557-564.

Schnurr K, Brinckmann R, and Kuhn H (1999) Cytokine Induced Regulation of 15-Lipoxygenase and Phospholipid Hydroperoxide Glutathione Peroxidase in Mammalian Cells. *Adv Exp Med Biol* **469**:75-81.

Serhan CN, Chiang N, and Van Dyke TE (2008) Resolving Inflammation: Dual Anti-Inflammatory and Pro-Resolution Lipid Mediators. *Nat Rev Immunol* **8**:349-361.

Sozzani S, Zhou D, Locati M, Bernasconi S, Luini W, Mantovani A, and O'Flaherty JT (1996) Stimulating Properties of 5-Oxo-Eicosanoids for Human Monocytes: Synergism With Monocyte Chemotactic Protein-1 and -3. *J Immunol* **157**:4664-4671.

Tai HH, Tong M, and Ding Y (2007) 15-Hydroxyprostaglandin Dehydrogenase (15-PGDH) and Lung Cancer. *Prostaglandins Other Lipid Mediat* **83**:203-208.

Viita H, Markkanen J, Eriksson E, Nurminen M, Kinnunen K, Babu M, Heikura T, Turpeinen S, Laidinen S, Takalo T, and Ylä-Herttuala S (2008) 15-Lipoxygenase-1 Prevents Vascular Endothelial Growth Factor A- and Placental Growth Factor-Induced Angiogenic Effects in

Rabbit Skeletal Muscles Via Reduction in Growth Factor MRNA Levels, NO Bioactivity, and Downregulation of VEGF Receptor 2 Expression. *Circ Res* **102**:177-184.

Walther M, Wiesner R, and Kühn H (2004) Investigations into Calcium-Dependent Membrane Association of 15-Lipoxygenase-1. Mechanistic Roles of Surface-Exposed Hydrophobic Amino Acids and Calcium. *J Biol Chem* **279**:3717-3725.

Weibel GL, Joshi MR, Alexander ET, Zhu P, Blair IA, and Rothblat GH (2009) Overexpression of Human 15(S)-Lipoxygenase-1 in RAW Macrophages Leads to Increased Cholesterol Mobilization and Reverse Cholesterol Transport. *Arterioscler Thromb Vasc Biol* Mar 26. [Epub ahead of print]; DOI:10.1161/ATVBAHA.109.186163.

Wittwer J and Hersberger M (2007) The Two Faces of the 15-Lipoxygenase in Atherosclerosis. *Prostaglandins Leukot Essent Fatty Acids* **77**:67-77.

Zhu P, Oe T, and Blair IA (2008) Determination of Cellular Redox Status by Stable Isotope Dilution Liquid Chromatography/Mass Spectrometry Analysis of Glutathione and Glutathione Disulfide. *Rapid Commun Mass Spectrom* **22**:432-440.

## FOOTNOTE

This work was supported by the National Institutes of Health [RO1CA091016 and P30ES013508].

## LEGENDS FOR FIGURES

Fig. 1: **Chemical structures of AA metabolites with similar structural features.**

Fig. 2: **LC-MRM/MS analysis of 15-LO-derived eicosanoids from primary human monocytes treated with AA and CI.** Primary human monocytes were isolated and stimulated with IL-4 for 40 h (**NT**) followed by 40 min treatment with 50 μM AA (**AA**) or 5 μM CI (**CI A-23187**). Cell supernatant in each treatment group was collected. Lipid metabolites in the cell supernatant were extracted, derivatized with PFB, and analyzed by stable isotope dilution LC-ECAPCI/MRM/MS analysis. MRM chromatograms are shown for (A) 15-(*R*,*S*)-HETE-PFB (*m/z* 319 → 219) and (B) 15-oxo-ETE-PFB (*m/z* 317 → 273).

Fig. 3: **LC-MRM/MS analysis and quantitation of 15-LO-derived eicosanoids from R15L cells and RMock cells treated with AA. (A)** Representative chromatograms of 15-LO-derived lipid metabolites released by R15L cells following 5 min treatment with 10 μM AA. MRM chromatograms are shown for (a) 15-oxo-ETE-PFB (*m/z* 317 → 273), (b) [$^2H_6$]-5-oxo-ETE-PFB internal standard (*m/z* 326 → 279), (c) 15-(*R*,*S*)-HETE-PFB (*m/z* 319 → 219), and (d) [$^2H_8$]-15-(*S*)-HETE-PFB internal standard (*m/z* 327 → 226); **(B)** Concentration-time graph of 15-HETE (*R* and *S*-form) released by R15L or RMock cells treated with 10 μM AA for 24 h; **(C)** Concentration-time graph of 15-oxo-ETE released by R15L or RMock cells treated with 10 μM AA for 24 h. Cell supernatants were collected at each time point. Lipid metabolites in the cell

supernatants were extracted and derivatized with PFB. Determinations were conducted in triplicate (means ± S.E.M.) by stable isotope dilution chiral LC-ECAPCI/MRM/MS analyses of PFB derivatives.

Fig. 4: **LC-MRM/MS analysis and quantitation of 15-LO-derived eicosanoids from R15L cells treated with CI. (A)** Representative chromatograms of endogenous 15-LO-derived lipid metabolites released by R15L cells following 40 min treatment with 5 μM CI. MRM chromatograms are shown for (a) 15-oxo-ETE-PFB (*m/z* 317 → 273), (b) [$^2H_6$]- 5-oxo-ETE-PFB internal standard (*m/z* 326 → 279), (c) 15-(*R*,*S*)-HETE-PFB (*m/z* 319 → 219), and (d) [$^2H_8$]-15-(*S*)-HETE-PFB internal standard (*m/z* 327 → 226); **(B)** Concentration-time graph of 15-HETE (*R* and *S*-form) released by R15L treated with 5 μM CI for 24 h; **(C)** Concentration-time graph of 15-oxo-ETE released by R15L cells treated with 5 μM CI for 24 h. Cell supernatants were collected at each time point. Lipid metabolites in the cell supernatants were extracted and derivatized with PFB. Determinations were conducted in triplicate (means ± S.E.M.) by stable isotope dilution chiral LC-ECAPCI/MRM/MS analyses of PFB derivatives.

Fig. 5: **Effect of LO inhibitor (CDC) on formation of 15-oxo-ETE and 15(S)-HETE by R15L cells.** (**A**) 15-Oxo-ETE formation by cells that were treated with 10 μM AA or pre-treated with 20 μM CDC for 40 min prior to vehicle or 10 μM AA treatment. **(B)** 15-Oxo-ETE formation by cells that were treated with 5 μM CI or pre-treated with 20 μM CDC for 40 min prior to vehicle or 5 μM CI treatment. (**C**) 15(*S*)-HETE

formation by cells that were treated with 10 μM AA or pre-treated with 20 μM CDC for 40 min prior to vehicle or 10 μM AA treatment. **(D)** 15(*S*)-HETE formation by cells that were treated with 5 μM CI or pre-treated with 20 μM CDC for 40 min prior to vehicle or 5 μM CI treatment. Lipid metabolites in the cell media were extracted and derivatized with PFB. 15-Oxo-ETE and 15(S)-HETE concentrations were determined in triplicate by stable isotope dilution LC-ECAPCI/MRM/MS analyses of PFB derivatives. Values presented in bar graphs are means ± S.E.M.

Fig. 6: **Kinetics of 15(*S*)-HETE metabolism by R15L cells.** R15L cells were incubated with 15(*S*)-HETE (1 μM) for a period of 360 min. Supernatant was collected at different time points. Lipid metabolites [15(*S*)-HETE and 15-oxo-ETE] in the cell supernatant were extracted and derivatized with PFB and their concentrations were determined in triplicate (means ± S.E.M.) by LC-ECAPCI/MRM/MS analysis. **(A)** Concentration-time plot of 15(*S*)-HETE (μM) remaining un-metabolized in R15L cell culture media; **(B)** Kinetic plot of 15(*S*)-HETE metabolism by R15L cells ($t_{1/2}$=21 min and k=0.0331 $min^{-1}$); **(C)** Concentration-time plot of 15-oxo-ETE (μM) produced in R15L cell culture media. (D) Kinetic plot of 15-oxo-ETE metabolism by R15L cells ($t_{1/2}$=11 min and k=0.0643 $min^{-1}$).

Fig. 7: **Dose-dependent effects of CAY10397 on the levels of 15-oxo-ETE and 15(*S*)-HETE released by R15L cells. (A)** Dose-dependent inhibition curve of CAY10397 on 15-oxo-ETE released by R15L cells treated with 10 μM AA for 10 min following the pretreatment with CAY10397 for 4 h; **(B)** Dose-dependent curve of CAY10397

on 15(*S*)-HETE accumulation by R15L cells treated with 10 μM AA for 10 min following the pretreatment with CAY10397 for 4 h; **(C)** Dose-dependent inhibition curve of CAY10397 on 15-oxo-ETE released by R15L cells treated with 50 nM 15(*S*)-HETE for 10 min following the pretreatment with CAY10397 for 4 h; **(D)** Dose-dependent curve of CAY10397 on 15(*S*)-HETE accumulation by R15L cells treated with 50 nM 15(*S*)-HETE for 10 min following the pretreatment with CAY10397 for 4 h. Cell supernatants were collected at each time point. Lipid metabolites in the cell supernatants were extracted and derivatized with PFB. Determinations were conducted in triplicate (means ±S EM) by stable isotope dilution chiral LC-ECAPCI/MRM/MS analyses of PFB derivatives.

Fig. 8: **Effect of 15-oxo-ETE on cell proliferation of HUVECs.** Determinations were conducted in triplicate (means ± S.E.M.). Concentrations of 15-oxo-ETE were determined by LC-ECAPCI/MS. (**A)** HUVECs were treated with various doses (0-20 μM) of 15-oxo-ETE for a period of 48 h. Cell proliferation in terms of DNA synthesis was determined by colorimetric BrdU ELISA assays. Absorbance was measured at 370 nm in triplicate and the corresponding cell number was determined from a standard curve. (**B**) Intracellular levels of 15-oxo-ETE in HUVECs incubated with 1 μM 15-oxo-ETE for 48 h. (**C**) Intracellular levels of 15-oxo-ETE in HUVECs incubated with 10 μM 15-oxo-ETE for 48 h.

Fig. 9: **Formation and action of 15-LO-1-derived eicosanoids in a monocyte/macrophage cell model.** IL-4 binds to its receptor, and activates JAK1,

Molecular Pharmacology Fast Forward. Published on June 17, 2009 as DOI: 10.1124/mol.109.057489
This article has not been copyedited and formatted. The final version may differ from this version.



which causes dimerization and nuclear trans-localization of transcription 6 (Stat6). The dimerized Stat6 binds to DNA stimulating the production of 15-LO-1. When intracellular calcium concentrations increase, 15-LO-1 is recruited to the inner side of the cell membrane where metabolizes AA to 15(*S*)-HPETE and 15(*S*)-HETE which is released by c-$PLA_2$ from the plasma membrane. 15(*S*)-HETE is then oxidized to 15-oxo-ETE by intracellular 15-PGDH and 15-oxo-ETE is conjugated to form OEG, which is released and hydrolyzed by GGTP to give OEC. Released intact 15-oxo-ETE can participate in cell-cell interactions such as with ECs to inhibit proliferation.

Molecular Pharmacology Fast Forward. Published on June 17, 2009 as DOI: 10.1124/mol.109.057489
This article has not been copyedited and formatted. The final version may differ from this version.

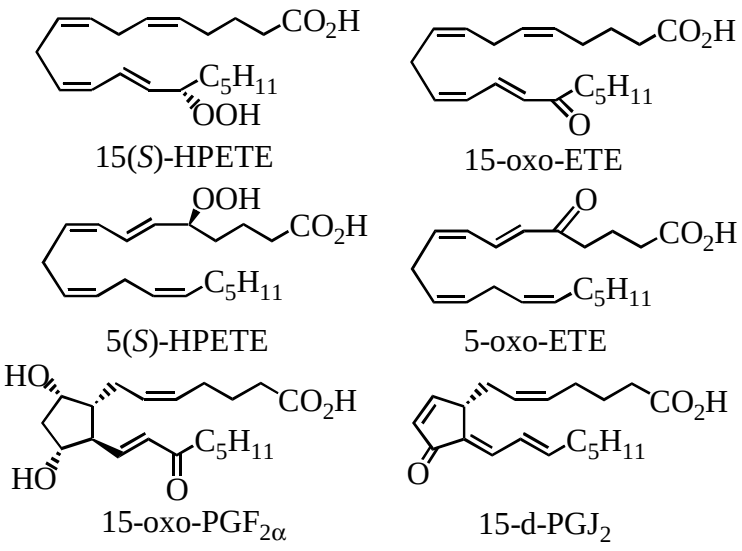


Figure 1

Molecular Pharmacology Fast Forward. Published on June 17, 2009 as DOI: 10.1124/mol.109.057489
This article has not been copyedited and formatted. The final version may differ from this version.

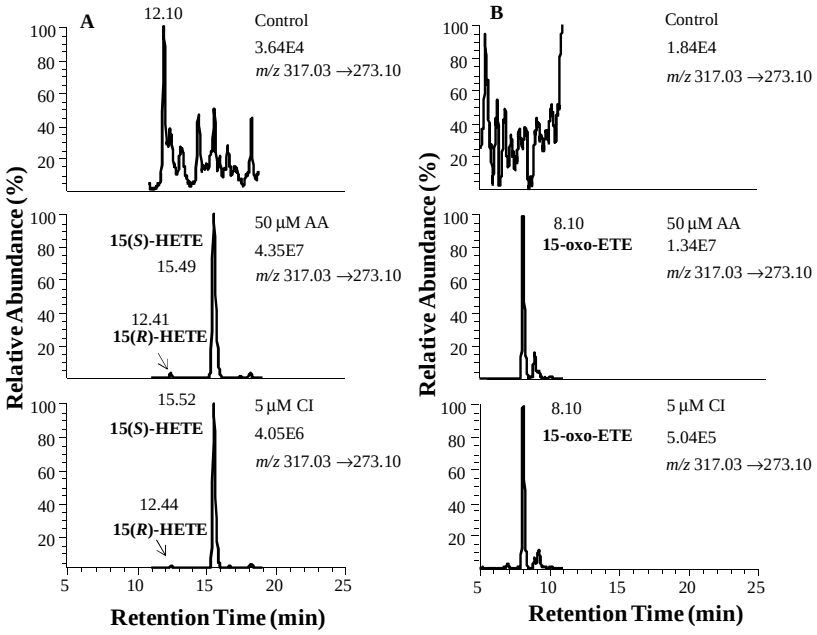


Figure 2

Molecular Pharmacology Fast Forward. Published on June 17, 2009 as DOI: 10.1124/mol.109.057489
This article has not been copyedited and formatted. The final version may differ from this version.

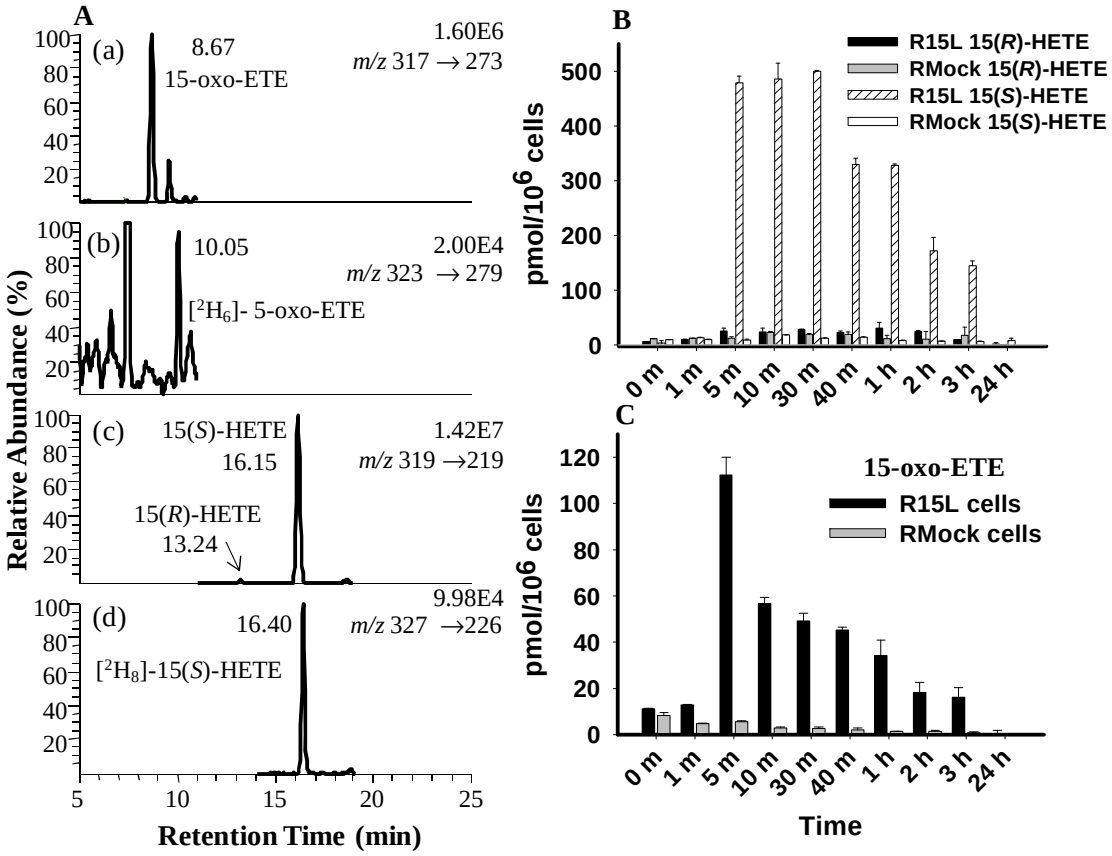


Figure 3

Molecular Pharmacology Fast Forward. Published on June 17, 2009 as DOI: 10.1124/mol.109.057489
This article has not been copyedited and formatted. The final version may differ from this version.

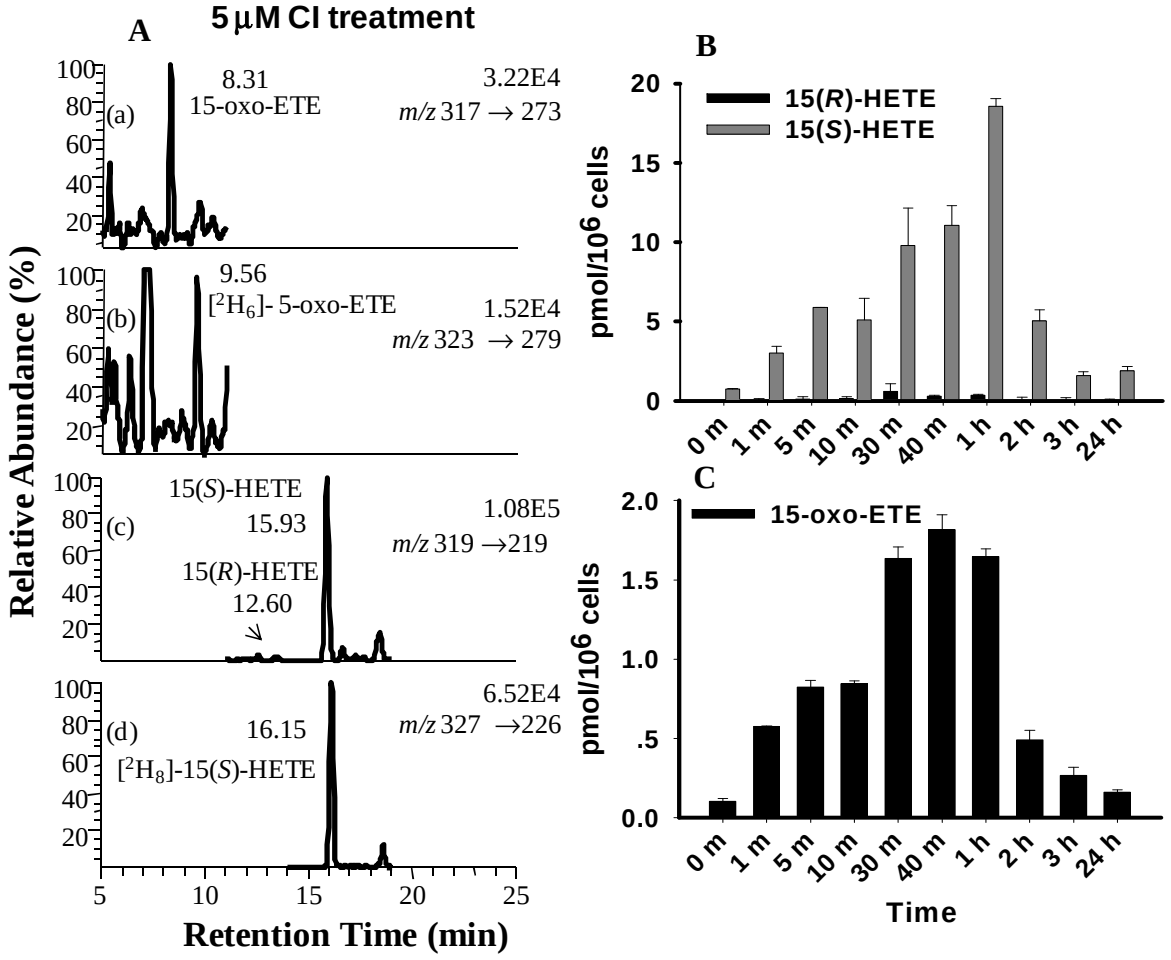


Figure 4

Molecular Pharmacology Fast Forward. Published on June 17, 2009 as DOI: 10.1124/mol.109.057489
This article has not been copyedited and formatted. The final version may differ from this version.

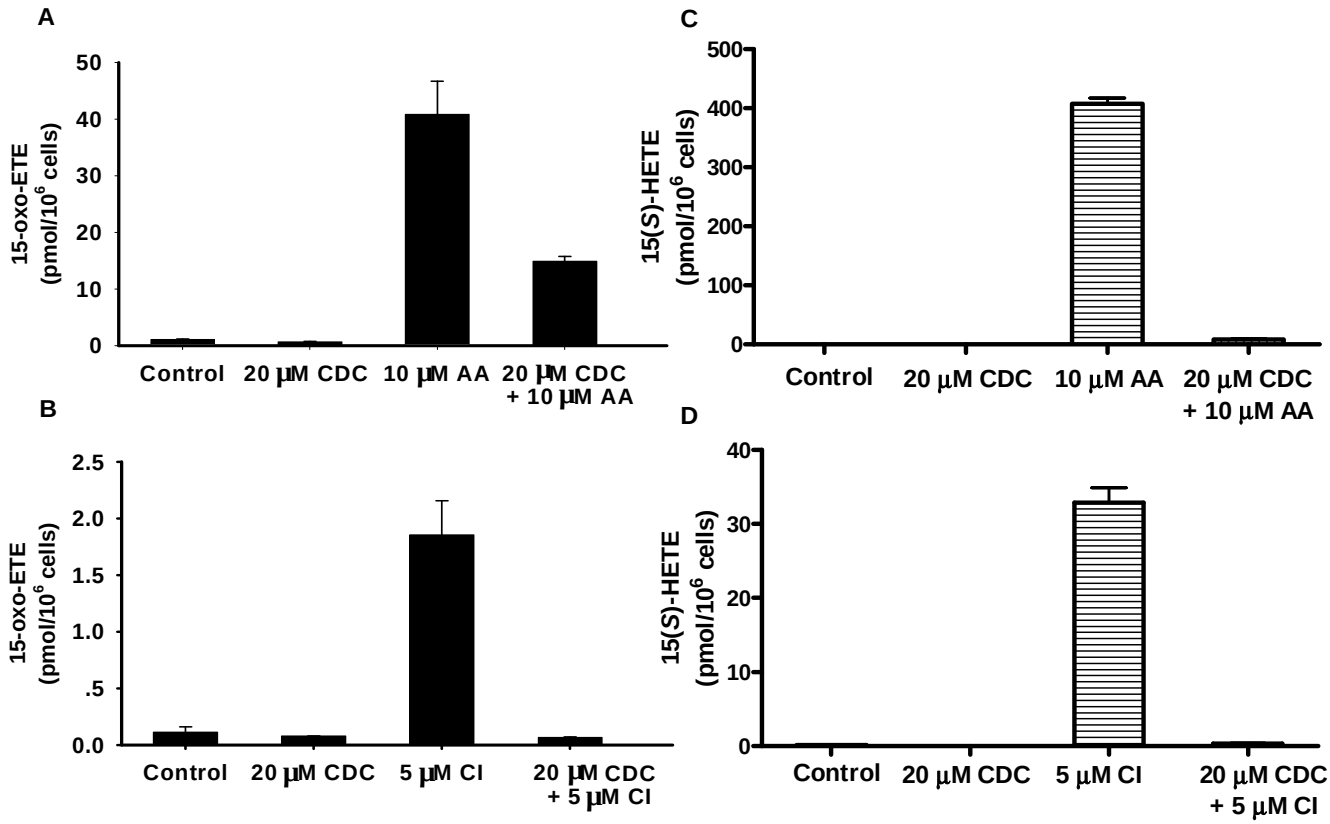


Figure 5

Molecular Pharmacology Fast Forward. Published on June 17, 2009 as DOI: 10.1124/mol.109.057489
This article has not been copyedited and formatted. The final version may differ from this version.

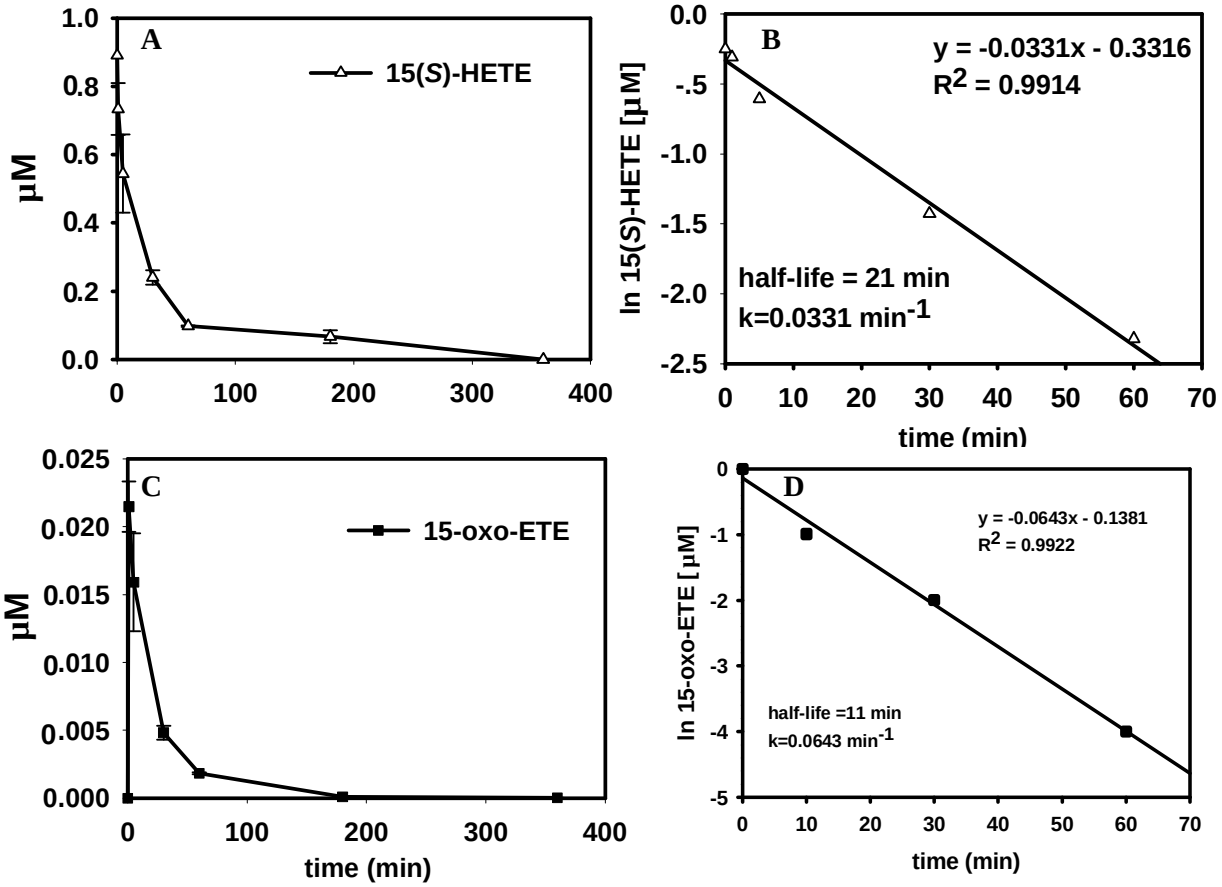


Figure 6

Molecular Pharmacology Fast Forward. Published on June 17, 2009 as DOI: 10.1124/mol.109.057489
This article has not been copyedited and formatted. The final version may differ from this version.

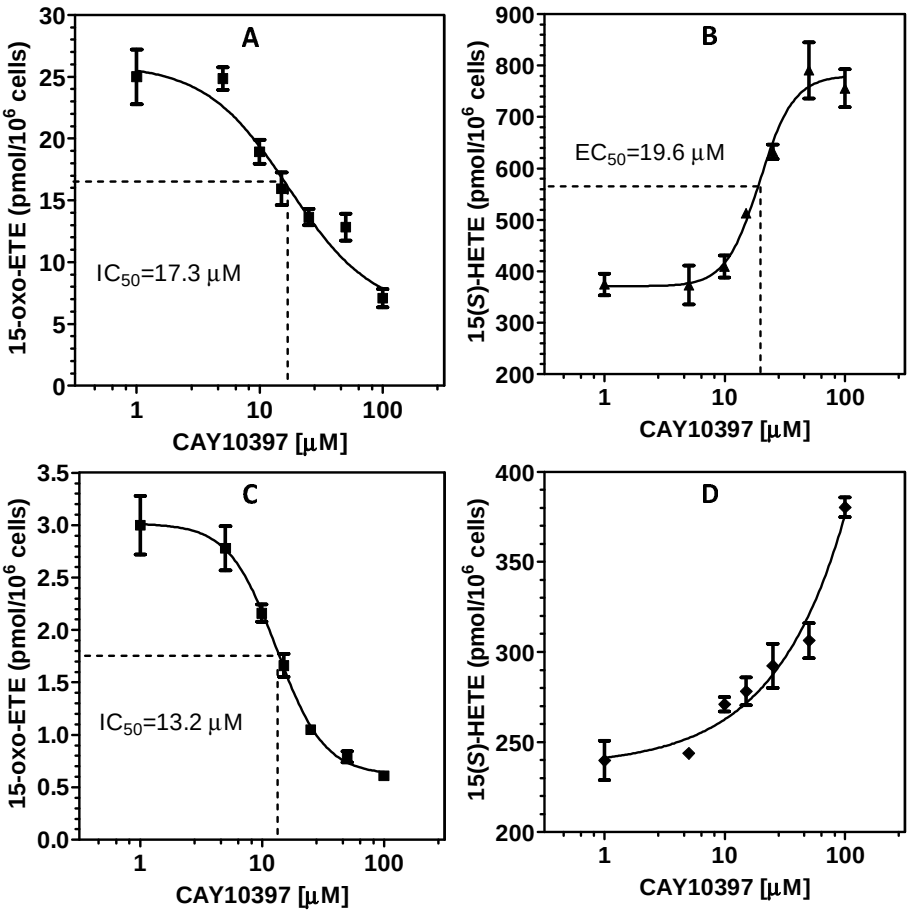


Figure 7

Molecular Pharmacology Fast Forward. Published on June 17, 2009 as DOI: 10.1124/mol.109.057489
This article has not been copyedited and formatted. The final version may differ from this version.

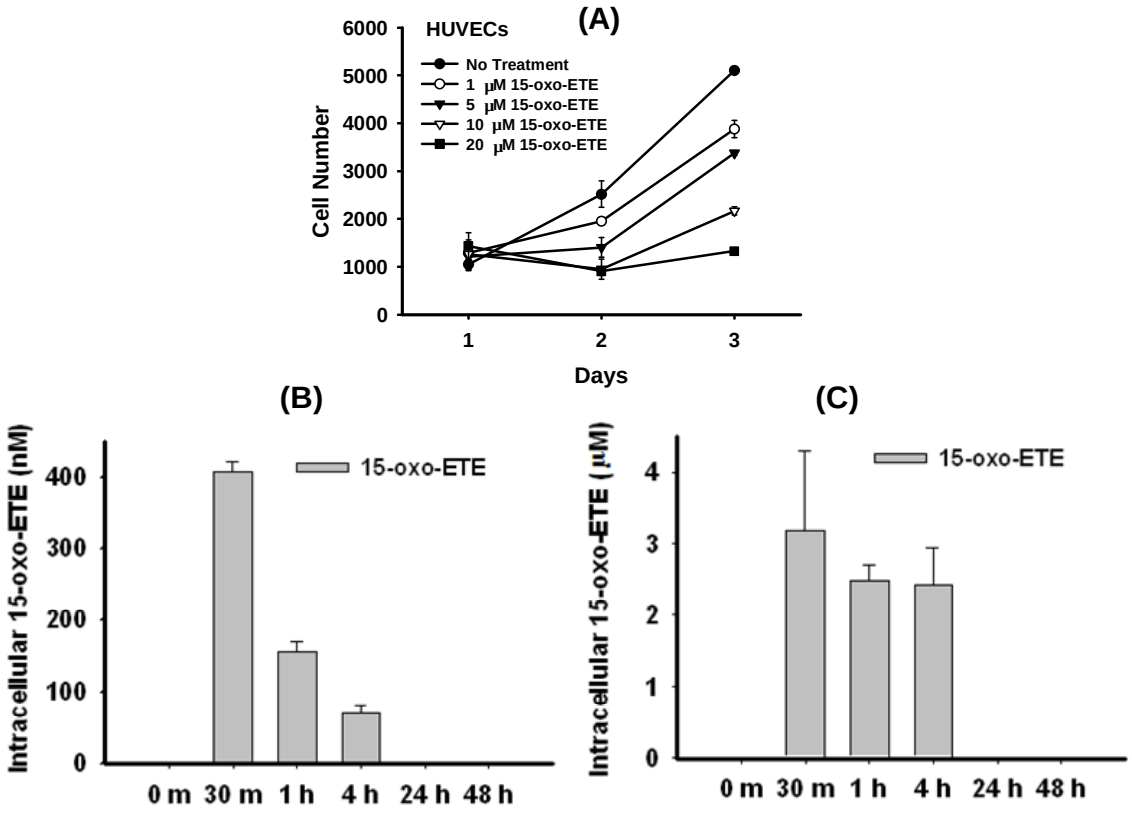


Figure 8

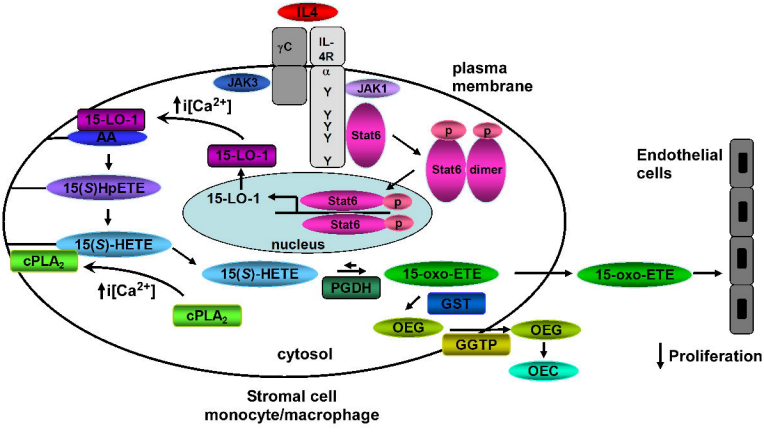
IL4
γC
IL-4R
α
Y
Y Y Y Y
Y
JAK3
JAK1
plasma membrane
↑i[Ca2+]
15-LO-1
AA
15-LO-1
Stat6
P
P
Stat6 dimer
Endothelial cells
15(S)HpETE
15-LO-1
Stat6
P
Stat6
P
nucleus
15(S)-HETE
cPLA2
15(S)-HETE
PGDH
15-oxo-ETE
15-oxo-ETE
↑i[Ca2+]
cPLA2
GST
OEG
GGTP
OEG
OEC
cytosol
↓Proliferation
Stromal cell
monocyte/macrophage

Figure 9